Delft University of Technology

Direct Water Injection in Catholyte-Free Zero-Gap Carbon Dioxide Electrolyzers

De Mot, Bert; Ramdin, Mahinder; Hereijgers, Jonas; Vlugt, Thijs J.H.; Breugelmans, Tom

Important note
To cite this publication, please use the final published version (if applicable).
Please check the document version above.

Direct Water Injection in Catholyte-Free Zero-Gap Carbon Dioxide Electrolyzers

Bert De Mot,*[a] Mahinder Ramdin,[b] Jonas Hereijgers,[a] Thijs J. H. Vlugt,[b] and
Tom Breugelmans*[a, c]

A zero-gap flow electrolyzer with a tin-coated gas diffusion electrode as the cathode was used to convert humidified gaseous CO_2 to formate. The influence of humidification, flow pattern and the type of membrane on the faradaic efficiency (FE), product concentration, and salt precipitation were investigated. We demonstrated that water management in the gas diffusion electrode was crucial to avoid flooding and (bi)carbonate precipitation, to uphold a high FE and formate concentration. Direct water injection was validated as a novel approach for water management. At 100 mA/cm^2, direct water injection in combination with an interdigitated flow channel resulted in a FE of 80% and a formate concentration of 65.4 +/−0.3 g/l without salt precipitation for a prolonged CO_2 electrolysis of 1 h. The use of bipolar membranes in the zero-gap configuration mainly produced hydrogen. These results are important for the design of commercial scale CO_2 electrolyzers.

Electrochemical reduction of CO_2 to useful chemicals is an interesting example of carbon capture and utilization (CCU).[1–3] A tremendous effort has been made to better understand the effects of different parameters (e.g., temperature, pressure, electrolyte, type and morphology of catalysts, impurities, membranes, cell configuration, etc.) on the CO_2 reduction reaction (CO2RR).[4–8] The current status of the CO2RR is that only small molecules like carbon monoxide (CO),[9] formate ($HCOO^-$)[10–15] and ethylene (C_2H_4)[16,17] can be obtained with high Faradaic efficiencies (FEs) and current densities (CDs). It is also clear that the CO2RR in the liquid phase is intrinsically limited by mass transfer and one has to rely on gas diffusion electrodes (GDEs) to achieve industrially relevant reaction rates (i.e., CDs > 100 mA/cm^2).[8,18–21]

[a] B. De Mot, Dr. J. Hereijgers, Prof. Dr. T. Breugelmans
     Research Group Applied Electrochemistry & Catalysis
     University of Antwerp
     Universiteitsplein 1, 2610 Wilrijk, Belgium
     E-mail: bert.demot@uantwerpen.be
            tom.breugelmans@uantwerpen.be
[b] Dr. M. Ramdin, Prof. Dr. T. J. H. Vlugt
     Engineering Thermodynamics, Process & Energy Department
     Faculty of Mechanical, Maritime and Materials Engineering
     Delft University of Technology
     Leeghwaterstraat 39, 2628CB Delft, The Netherlands
[c] Prof. Dr. T. Breugelmans
     Separation & Conversion Technologies
     VITO
     Boeretang 200, 2400 Mol, Belgium
     Supporting information for this article is available on the WWW under
     https://doi.org/10.1002/celc.202000961

A central problem in GDE-based CO2RR is the formation of salts at the cathode, which deteriorates the performance of the reactor.[22] Precipitation of (bi)carbonate occurs due to the reaction between the supplied CO_2 and the hydroxide ions generated at the cathode. Therefore, it is crucial to supply sufficient water to the cathode to prevent precipitation.[22–26] An excess of water will 1) dilute the product, which is undesired for downstream separation purposes,[27,28] and 2) cause flooding of the GDE, limiting mass transport of CO_2.[7,29] Currently, water is supplied to the CO_2 stream by bubbling the gas through a heated water reservoir, resulting in a saturated gas flow.[30–32] By adjusting the temperature of the water reservoir, the total amount of water in the saturated CO_2 gas stream can be controlled.[30] This process is relatively easy to implement on a lab scale, however, it has some major disadvantages: 1) inaccurate estimation of the total amount of water input (e.g. condensation in the feed tubes, change in temperature), 2) not applicable/practical on industrial-scale, and 3) cross influence of the gas stream temperature on the reactor performance. An improved water management system is primordial to allow the evolution from lab-scale electrolyzers to an industrial process.[6] In this work, we present direct water injection as an approach for water management in a zero-gap flow CO_2 electrolyzer with a tin-coated GDE for CO_2 conversion to formate. The effect of different parameters (i.e., humidification, flow channel pattern and membrane type) on the FE, formate concentration, and salt precipitation was investigated.

In state-of-the-art research of GDEs, water management is performed by bubbling CO_2 through a water reservoir. A more straightforward, accurate and up-scalable water management method is the direct injection of liquid water in the gas stream,[33] creating a gas/liquid mixed flow, as shown in Figure 1. The flow of CO_2 was controlled by a mass flow controller (Brooks instruments, GF040) and the flow of injected water was adjusted with a HPLC pump (Watrex, P102). A T-mixer was used to mix the gas and the liquid. The mixed flow was fed to a zero-gap electrolyzer, with a Ni-Foam/Nafion117/Sn-GDE membrane electrode assembly (MEA). The humidified CO_2 reacted towards formate at the catalyst surface of the Sn-GDE. A detailed description of the materials and methods can be found in the supporting information (SI 1 and SI 8).

The performance of the zero-gap electrolyzer was compared to the well-known catholyte flow-by electrolyzer, which has been described in our previous work.[34] The major difference between these configurations is the absence of a catholyte flow channel in the zero-gap electrolyzer. For the zero-gap electrolyzer, two types of gas flow patterns were tested: a parallel pattern (Figure 2A), in which the mass transfer to the GDE

ChemElectroChem

Communications
doi.org/10.1002/celc.202000961

Chemistry Europe
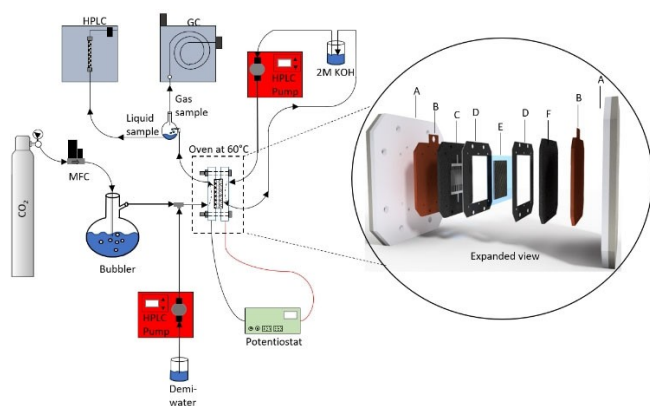European Chemical
Societies Publishing

Figure 1. Experimental set-up of the zero-gap electrolyzer with direct water injection for optimized water management. Expanded view: A) end-plates; B) current collectors; C) anode flow channel; D) gaskets; E) MEA; F) cathode flow channel.
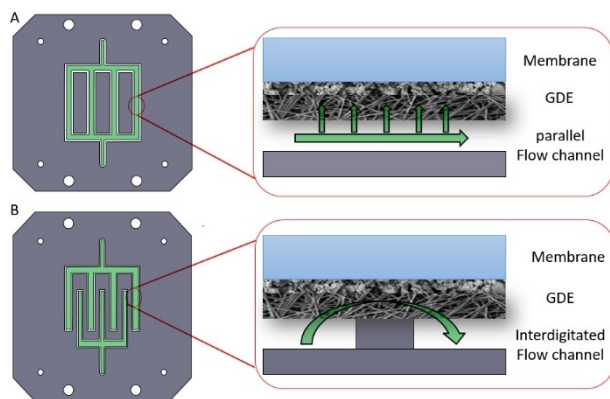

Figure 2. Schematic of the flow field patterns of the zero-gap electrolyzer: A) parallel pattern where mass transfer is due to diffusion and B) interdigitated pattern where mass transfer is a combination of diffusion and convection.

occurred only by diffusion, and an interdigitated pattern (Figure 2B), in which the mass transfer occurred both by diffusion and convection. The experiments were executed for 1 h at 100 mA/cm². The CO_2 flowrate was 200 ml/min and 0.3 ml/min water was injected in the gas stream.

A clear distinction in terms of cell voltage between the three reactor lay-outs was observed (Figure 3A). The zero-gap reactor had a cell voltage of 3,1 V for the parallel and 2.7 V for the interdigitated flow channel, meanwhile, the flow-by reactor showed a cell voltage of 5.5 V, which is double the voltage of the interdigitated zero gap electrolyzer. To understand this, electrochemical impedance spectroscopy at open circuit potential was performed to measure the ohmic resistance of the different cells (SI 7). For the zero-gap electrolyzer, an ohmic resistance of 0.28 Ω (interdigitated) and 0.38 Ω (parallel) was measured while the flow-by electrolyzer showed an ohmic resistance of 1.45 Ω, Consequently, the tremendous difference in cell voltage observed in Figure 3A can be attributed to the higher ohmic resistance of the flow-by reactor due to the presence of a 0.5 M $KHCO_3$ layer between the cathode and the membrane

Furthermore, a difference between the parallel and interdigitated flow channel of the zero-gap electrolyzer was noted: the interdigitated pattern had a 0.5 V lower cell voltage and was significantly more stable than the parallel flow channel, in which the cell response had potential spikes up to several hundred millivolts. Considering that 1) in the parallel flow pattern mass transfer occurred exclusively through diffusion and 2) the hydrophobicity of the GDE, the authors suggest that most of the water injected in the cell did not reach the catalyst surface. This led to a poor humidification of the MEA, which decreased its ionic conductivity and caused poor product removal. Due to the accumulation of products at the catalyst surface, voltage spikes were observed. This behavior was observed in multiple repeating experiments and was not the result of a 'one-time' faulty MEA. In sharp contrast, when the interdigitated flow channel was used, CO_2 was forced into the GDE and the mass transfer towards the catalyst surface was
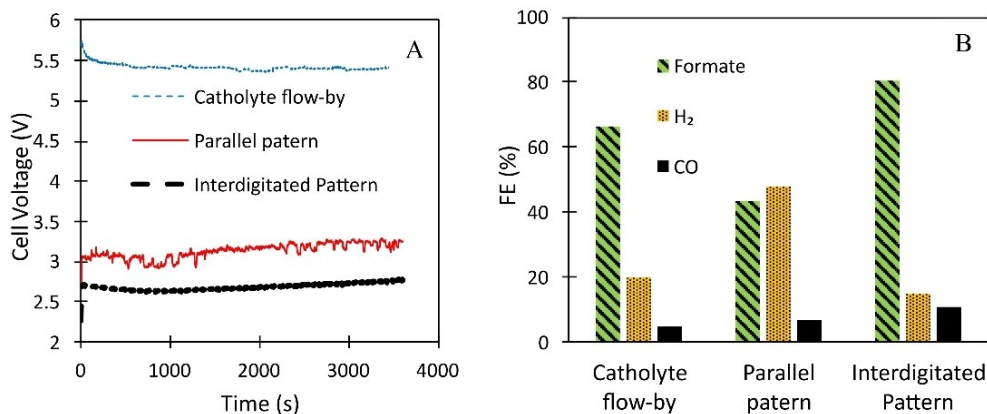

Figure 3. A) Chronopotentiometric curve recorded at 100 mA/cm² for 1 h with a CO_2 flowrate of 200 ml/min and a temperature of 60 °C for: an interdigitated zero-gap electrolyzer (black/dashed); a parallel zero-gap electrolyzer (red/solid) and a catholyte flow-by electrolyzer (blue/dotted). B) FE's of the products analyzed: formate (dashed); H_2 (dotted) and CO (solid). The flow-by electrolyzer was fed with 20 ml/min 0.5 M $KHCO_3$ on the cathode side and 20 ml/min 2 M KOH on the anolyte side. The Zero- gap electrolyzers were fed with 0.3 ml/min water, injected in the CO_2 flow on cathode side and 20 ml/min 2 M KOH on the anolyte side.

thus a combination of both diffusion and convection. Moreover, water was also pushed into the GDE, resulting in a more effective humidification of the MEA. Due to the optimized water transport, the accumulation of reaction products was prevented and no voltage spikes were observed. Furthermore, it was noted that the GDE showed no structural damage after forcing water in its pores. It is suggested that this is mainly due to the electrowetting effect[22,34] and the decreased surface tension due to formate production.[25] The results of the product analysis (Figure 3B) showed an average $FE_{formate}$ of 67% when the catholyte flow-by electrolyzer was used, which was in line with our previous work.[34] The side products were mainly H_2 (25%) and to lesser extent CO (5%). The cumulative FE was 97 +/−3.2%, proving the analysis methods were accurate. Regarding the zero-gap electrolyzer, yet again, a big difference was observed between the interdigitated flow pattern, 81% $FE_{formate}$, and the parallel flow pattern, 43% $FE_{formate}$. This could once more be attributed to the increased mass transfer and humidification performance of the interdigitated channel resulting in a better CO_2 transport and wettability of the MEA.

One of the major disadvantages of interdigitated flow patterns is the increased energy cost, caused by higher pressure drops required to push the gas through the GDE.[35] The observed pressure drops during the experiments where 50 mbar (interdigitated) compared to 20 mbar (parallel). This results in only a minimal power increase of the overall system which is more than compensated by the lower cell voltage of the interdigitated based electrolyzer as shown in Figure 3A.

Additionally, the influence of the membrane type was investigated (Nafion versus bipolar membrane) these results can be found in the supporting information (SI 4).

As discussed, insufficient water supply in the electrolyzer leads to salt precipitation, while an excess of water results in decreased concentration of the liquid products. Therefore, optimization of the water flowrate is a crucial step in the optimization of electrolyzers. The minimum amount of water injection that is required to prevent salt precipitation in the cathode compartment can be calculated from the water balance (Eq.1):

$$F_w^{inj}. = S - F_w^{g,in} + F_w^{g,out} - F_w^{drag} + F_w^{diff} + r_w \tag{1}$$

Where F_w^{inj} is the amount of injected water, S is the minimum amount of water required for solubilizing the salts, F_w^{drag} the amount of water dragged through the membrane due to electro-osmosis, F_w^{diff} the amount of water transported from the cathode due to back-diffusion, r_W the amount of water consumed in the reactions, $F_w^{g,in}$ and $F_w^{g,out}$ are the amounts of gaseous water present in the CO_2 stream entering and leaving the cell. The amount of water transported due to back-diffusion and the saturated CO_2 streams can be neglected, as explained in the Supporting Information (SI 2). Therefore, the required amount of water injection mainly depends on the solubility of the salts, the electro-osmotic drag coefficient, and the consumption of water due to reactions. At the cathode, potassium formate and potassium bicarbonate are formed, thus the amount of water in the cathode compartment should exceed the combined solubility limit of both salts to avoid crystalliza-

tion. It was calculated (SI 2) that a minimum water flow ($=S$) of 0.11 ml/min is necessary to remove all the salts formed at 100 mA/cm². The amount of water consumed by the reactions can be obtained from the CO2RR (Eq.2) and the HER (Eq.3).

$$CO_2 + 2e^- + H_2O \rightarrow HCOO^- + OH^- \tag{2}$$

$$2H_2O + 2e^- \rightarrow H_2 + 2OH^- \tag{3}$$
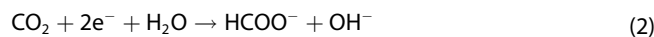
If an 80% FE towards formate is assumed at 100 mA/cm², using Faraday's law, this results in a combined water consumption ($=r_W$) of 0.011 ml/min. The amount of water transported due to electro-osmotic drag can be estimated from Eq.4:

$$F_w^{drag} = (A^* i^* n_d)/F \tag{4}$$

Where A is the area of the membrane, i the current density, n_d the electro-osmotic drag coefficient, and F the Faraday's constant. The electro-osmotic drag coefficient for Nafion 117 has been reported in the literature.[36,37] Using Eq. 4. an F_w^{drag} of 0.018 ml/min was calculated for a constant current of 100 mA/cm² and a n_d of 1 (SI 2). By submitting the calculated results for S, F_w^{drag} and r_W into Eq. 1, the total amount of additional water that has to be injected to prevent crystallization ($=F_w^{inj}$) was calculated as 0.15 +/−0.05 ml/min. To validate this theoretical minimum injection flowrate, experiments were performed with a water injection flow rate varying between 0.1 ml/min and 1 ml/min while using the zero-gap electrolyzer equipped with an interdigitated flow channel.

Running the experiment at 0.1 ml/min initially gave good performance with an average FE towards formate of 87% and a cell potential of 2.77 V (Figure 4A). However, after 50 minutes the pressure in the gas channel rose rapidly, causing the experiment to be stopped. After disassembling the cell, large clusters of crystalized salts were identified in the gas channel, completely blocking the passage of CO_2 (Figure S3). When the water injection flow rate was increased to 0.2 ml/min, a 1 h experiment could be finished without any visual salt deposits, validating the theoretical value calculated using Eq. 1. Post-experiment analysis of the GDE's using ICP-MS (SI 10) showed that the amount of salt left in the GDE drastically decreased at higher flowrates, thereby demonstrating more efficient salt removal at these flowrates.

In addition, it was noted that an increased water flow rate did not had a substantial impact on both the FE towards formate and the cell potential, as all values were situated around 80% and 2.7 V respectively. However, a major difference was recorded when the concentration of the final product was analyzed (Figure 4B). At the lowest flow rate, a formate concentration of 95 g/l was achieved. As discussed earlier, this result was only stable for 50 minutes due to salt precipitation. At 0.2 ml/min, a constant formate concentration of 65 g/l was reached over the course of 60 minutes. Hence, upon increasing the water flow rate, the formate concentration decreased. At 1.0 ml/min, the formate concentration was only 18 g/l. To compare these results to current research on zero-gap formate production, a figure is added to the supporting information (SI 9), in which the partial current density
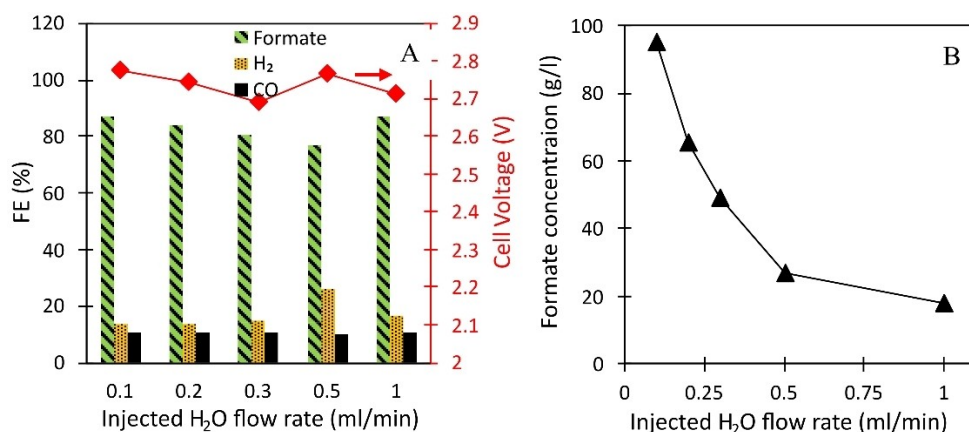
ChemElectroChem

Communications
doi.org/10.1002/celc.202000961

**Chemistry
Europe**
European Chemical
Societies Publishing

Figure 4. A) Average FE towards formate and cell voltage of an interdigitated based zero-gap electrolyzer at 100 mA/cm² and water injection flow rates varying between 0.1 and 1 ml/min at a CO_2 flowrate of 200 ml/min for 1 h, 20 ml/min 2 M KOH was fed to the anode side of the cell. B) Effect of water injection flow rate on formate concentration.

versus the formate concentration is plotted. From this figure it can be clearly seen that the data presented above is similar to current state of the art, with the addition of a more straightforward up-scaling perspective and more accurate controllability of the water flow rate.

To determine the long-term performance of the zero-gap electrolyzer a 25 h stability experiment was performed in both chrono potentiometric (100 mA/cm²) and chrono amperometric mode (2.7 V). Operating in chrono potentiometric mode (Figure 5A) it can be clearly seen that the cell voltage increased drastically after the first hour from 2.6 to 3.1 V causing a rapid increase of hydrogen evolution and a decrease in the $FE_{Formate}$ to 30%. After the initial drop the cell voltage kept decreasing slowly, this was due to the depletion of OH^- ions in the anolyte, increasing the overpotential at anode side. Refreshing the anolyte at the 17th hour clearly showed a recovering in both the cell voltage and the FE, after which it slowly decreased again. To prevent an increase of cell voltage overtime, the experiment was repeated in chrono amperometric mode, at 2.7 V, Figure 5B . In the first hour, the cell operates well, achieving good FEs (85%) at high current densities (120 mA/cm²). After the first hour, both the current density and the FE dropped to 60 mA/cm² and 68%, respectively. Again, a slow degradation of current density was noted due to the depletion of hydroxide ions in the anolyte, refreshing the anolyte resulted in a temporary increase of current density, visible at the 7th hour and the 22nd hour.

The authors strongly feel that this behavior can be attributed to two main phenomena. Firstly, non-ideal flow distribution led to local flooding of the GDE. This behavior has previously been investigated in interdigitated based hydrogen fuel cells where it caused reduced mass transfer of the reacting species and unstable performance[35,38–40] Therefore more research on the optimization of the design parameters of the indigitated flow channel (channel/land width, channel depth, etc.) is necessary to obtain a long term stable performance. Secondly, due to the formation of hydroxide ions at the cathode, the pH rises and the side reaction of CO_2 towards carbonate is favored. Especially at higher current densities this
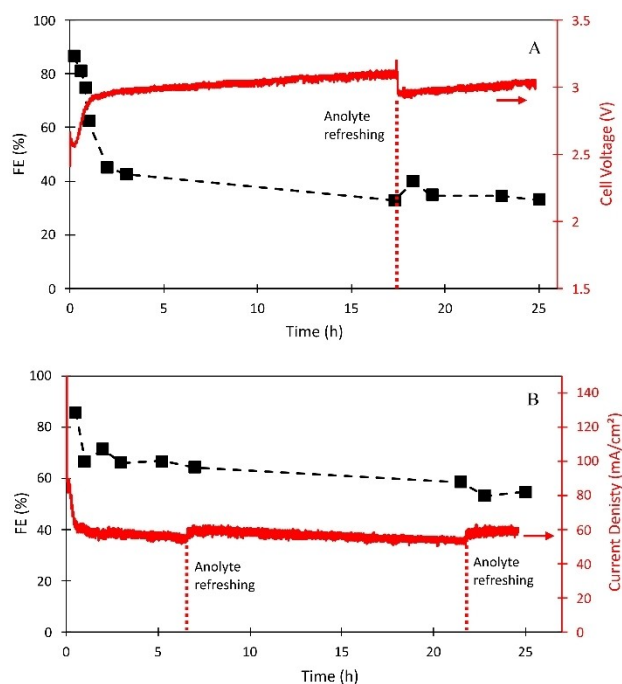

Figure 5. A) Long term stability (25 h) of an interdigitated based zero-gap electrolyzer operated in chrono potentiometric mode (100 mA/cm²), a water injection flow rate of 0.2 ml/min and a constant CO_2 flow of 200 ml/min. B) Long term stability (25 h) of an interdigitated based zero-gap electrolyzer operated in chrono amperometric mode (2.7 V), a water injection flow rate of 0.2 ml/min and a constant CO_2 flow of 200 ml/min. In both experiments, 2 M KOH was circulated at 20 ml/min on the anode side.

can lead to local CO_2 depletion at the catalyst surface where HER will dominate, as shown in Figure 5A.

In summary, direct water injection as a new method for the water management of a zero-gap CO_2 electrolyzer was validated and compared to the state-of-the-art catholyte flow-by electrolyzer. It was concluded that the zero-gap electrolyzer out-performed the catholyte flow-by electrolyzer, both on $FE_{formate}$ as on the cell voltage, overall resulting in a more efficient system. Furthermore, an interdigitated flow pattern outclassed

the parallel flow pattern due to the improved mass transfer of both CO_2 and water.

The effect of the amount of water injected on the cell performance was evaluated and compared to the theoretical minimal value calculated from the water balance. It was found that a minimum of 0.2 ml/min of water was necessary to prevent salt crystallization in the electrolyzer, resulting in a constant production of 60 g/l of formate at 2.7 V and 85% FE. Since the experimental data correlates almost perfectly with the theoretical equation provided in the manuscript (EQ 1), this equation can be directly used by experimentalists to calculate the required injection flowrate for their specific experimental set-up. Higher injection flow rate had no impact on the FE or the cell potential but a more diluted product was formed, 18 g/l of formate at 1 ml/min.

The long-term performance of the zero-gap electrolyzer was investigated in a 25 h experiment at both constant current and constant potential. The interdigitated channel shows a good performance but partial flooding of the GDE and neutralization of CO_2 limits the stability. Further optimization is required to acquire a more stable performance, which was not in the scope of this research.

Acknowledgements

Conflict of Interest

The authors declare no conflict of interest.

[1] H.-R. "Molly" Jhong, S. Ma, P. J. Kenis, *Curr. Opin. Chem. Eng.* **2013**, *2*, 191–199; Jhong, S. Ma, P. J. Kenis, *Curr. Opin. Chem. Eng.* **2013**, *2*, 191–199.
[2] C. Chen, J. F. Khosrowabadi Kotyk, S. W. Sheehan, *Chem* **2018**, *4*, 2571–2586.
[3] Z. J. Schiffer, K. Manthiram, *Joule* **2017**, *1*, 10–14.
[4] Q. Lu, F. Jiao, *Nano Energy* **2016**, *29*, 439–456.
[5] Y. Hori, H. Wakebe, T. Tsukamoto, O. Koga, *Electrochim. Acta* **1994**, *39*, 1833–1839.
[6] B. Endrödi, G. Bencsik, F. Darvas, R. Jones, K. Rajeshwar, C. Janáky, *Prog. Energy Combust. Sci.* **2017**, *62*, 133–154.
[7] O. G. Sánchez, Y. Y. Birdja, M. Bulut, J. Vaes, T. Breugelmans, D. Pant, *Curr. Opin. Green Sustain. Chem.* **2019**, DOI 10.1016/J.COGSC.2019.01.005.
[8] J. Song, H. Song, B. Kim, J. Oh, *Catalysts* **2019**, *9*, 224.
[9] N. Daems, B. De Mot, D. Choukroun, K. Van Daele, C. Li, A. Hubin, S. Bals, J. Hereijgers, T. Breugelmans, *Sustain. Energy Fuels* **2020**, *4*, 1296–1311.
[10] A. Del Castillo, M. Alvarez-Guerra, J. Solla-Gullón, A. Sáez, V. Montiel, A. Irabien, *Appl. Energy* **2015**, *157*, 165–173.
[11] E. Irtem, T. Andreu, A. Parra, M. D. Hernández-Alonso, S. García-Rodríguez, J. M. Riesco-García, G. Penelas-Pérez, J. R. Morante, *J. Mater. Chem. A* **2016**, *4*, 13582–13588.
[12] D. Kopljar, A. Inan, P. Vindayer, N. Wagner, E. Klemm, *J. Appl. Electrochem.* **2014**, *44*, 1107–1116.
[13] M. Ramdin, A. R. T. Morrison, M. de Groen, R. van Haperen, R. de Kler, E. Irtem, A. T. Laitinen, L. J. P. van den Broeke, T. Breugelmans, J. P. M. Trusler, et al., *Ind. Eng. Chem. Res.* **2019**, acs.iecr.9b03970.
[14] G. Díaz-Sainz, M. Alvarez-Guerra, J. Solla-Gullón, L. García-Cruz, V. Montiel, A. Irabien, *Catal. Today* **2018**, 1–7.
[15] C. Xia, P. Zhu, Q. Jiang, Y. Pan, W. Liang, E. Stavitsk, H. N. Alshareef, H. Wang, *Nat. Energy* **2019**, *4*, 776–785.
[16] C. T. Dinh, T. Burdyny, G. Kibria, A. Seifitokaldani, C. M. Gabardo, F. Pelayo García de Arquer, A. Kiani, J. P. Edwards, P. De Luna, O. S. Bushuyev, et al., *Science* **2018**, *360*, 783–787.
[17] L. Mandal, K. R. Yang, M. R. Motapothula, D. Ren, P. Lobaccaro, A. Patra, M. Sherburne, V. S. Batista, B. S. Yeo, J. W. Ager, et al., *ACS Appl. Mater. Interfaces* **2018**, *10*, 8574–8584.
[18] J.-B. Vennekoetter, R. Sengpiel, M. Wessling, *Chem. Eng. J.* **2019**, *364*, 89–101.
[19] C. Delacourt, P. L. Ridgway, J. B. Kerr, J. Newman, *J. Electrochem. Soc.* **2008**, *155*, DOI 10.1149/1.2801871.
[20] T. Burdyny, W. A. Smith, *Energy Environ. Sci.* **2019**, *12*, 1442–1453.
[21] D. Higgins, C. Hahn, C. Xiang, T. F. Jaramillo, A. Z. Weber, *ACS Energy Lett.* **2019**, *4*, 317–324.
[22] P. Jeanty, C. Scherer, E. Magori, K. Wiesner-Fleischer, O. Hinrichsen, M. Fleischer, *J. CO2 Util.* **2018**, *24*, 454–462.
[23] M. Duarte, B. De Mot, J. Hereijgers, T. Breugelmans, *ChemElectroChem* **2019**, *6*, 5596–5602.
[24] M. Leonard, L. E. Clarke, A. Forner-Cuenca, S. M. Brown, F. Brushett, *ChemSusChem* **2019**, cssc.201902547.
[25] M. Leonard, M. Orella, N. Aiello, Y. Román-Leshkov, A. Forner-Cuenca, F. Brushett, *J. Electrochem. Soc.* **2020**, *167*, 124521.
[26] G. Díaz-Sainz, M. Alvarez-Guerra, J. Solla-Gullón, L. García-Cruz, V. Montiel, A. Irabien, *AIChE J.* **2020**, *66*, DOI 10.1002/aic.16299.
[27] G. Díaz-Sainz, M. Alvarez-Guerra, J. Solla-Gullón, L. García-Cruz, V. Montiel, A. Irabien, *J. CO2 Util.* **2019**, *34*, 12–19.
[28] J. B. Greenblatt, D. J. Miller, J. W. Ager, F. A. Houle, I. D. Sharp, *Joule* **2018**, *2*, 381–420.
[29] P. Tiwari, G. Tsekouras, G. F. Swiegers, G. G. Wallace, *ACS Appl. Mater. Interfaces* **2018**, *10*, 28176–28186.
[30] W. Lee, Y. E. Kim, M. H. Youn, S. K. Jeong, K. T. Park, *Angew. Chem. Int. Ed.* **2018**, *57*, 6883–6887; *Angew. Chem.* **2018**, *130*, 6999–7003.
[31] C. M. Gabardo, C. P. O'Brien, J. P. Edwards, C. McCallum, Y. Xu, C.-T. Dinh, J. Li, E. H. Sargent, D. Sinton, *Joule* **2019**, DOI 10.1016/j.joule.2019.07.021.
[32] Y. C. Li, D. Zhou, Z. Yan, R. H. Gonçalves, D. A. Salvatore, C. P. Berlinguette, T. E. Mallouk, *ACS Energy Lett.* **2016**, *1*, 1149–1153.
[33] D. L. Wood, J. S. Yi, T. V. Nguyen, *Electrochim. Acta* **1998**, *43*, 3795–3809.
[34] B. De Mot, J. Hereijgers, M. Duarte, T. Breugelmans, *Chem. Eng. J.* **2019**, *378*, 122224.
[35] X.-D. Wang, Y.-Y. Duan, W.-M. Yan, X.-F. Peng, *Electrochim. Acta* **2008**, *53*, 5334–5343.
[36] S. Ge, B. Yi, P. Ming, *J. Electrochem. Soc.* **2006**, *153*, DOI 10.1149/1.2203934.
[37] F. Xu, S. Leclerc, D. Stemmelen, J. C. Perrin, A. Retournard, D. Canet, *J. Membr. Sci.* **2017**, *536*, 116–122.
[38] A. Aiyejina, M. K. S. Sastry, *J. Fuel Cell Sci. Technol.* **2012**, *9*, DOI 10.1115/1.4005393.
[39] N. J. Cooper, T. Smith, A. D. Santamaria, J. W. Park, *Int. J. Hydrogen Energy* **2016**, *41*, 1213–1223.
[40] J.-Y. Jang, C.-H. Cheng, Y.-X. Huang, *Int. J. Heat Mass Transfer* **2010**, *53*, 732–743.